Counteracting thermal degradation of LiPF6-based electrolyte with additives or lithium salts: A gas analysis revealing the impact of NMC

Baptiste Salomez, Sylvie Grugeon, Pierre Tran-Van, Stephane Laruelle

Journal of Power Sources 613 (2024) 234901

Contents lists available at ScienceDirect

Journal of Power Sources

journal homepage: www.elsevier.com/locate/jpowsour

Counteracting thermal degradation of $LiPF_6$-based electrolyte with additives or lithium salts: A gas analysis revealing the impact of NMC

Baptiste Salomez [a,c], Sylvie Grugeon [a,b], Pierre Tran-Van [c], Stephane Laruelle [a,b,*]

[a] Laboratoire de Réactivité et Chimie des Solides, CNRS, UMR 7314, Université de Picardie Jules Verne, 33 Rue Saint Leu, 80039, Amiens, France
[b] Réseau sur le Stockage Electrochimique de L'Energie, CNRS RS2E FR3459, France
[c] Renault, Ampère - Electric Components Division, Technocentre, 1 Avenue du Golf, 78288, Guyancourt, France

HIGHLIGHTS

- CO_2 gas analysis as a very sensitive tool to study electrolyte thermal degradation.
- N-containing additives are effective for PF_5-complexing in electrolyte alone.
- PF_5 adsorbs onto the NMC surface, preventing electrolyte solvents degradation.
- LiFSI hydrolysis leads to LiODFB decomposition, generating gas.

GRAPHICAL ABSTRACT

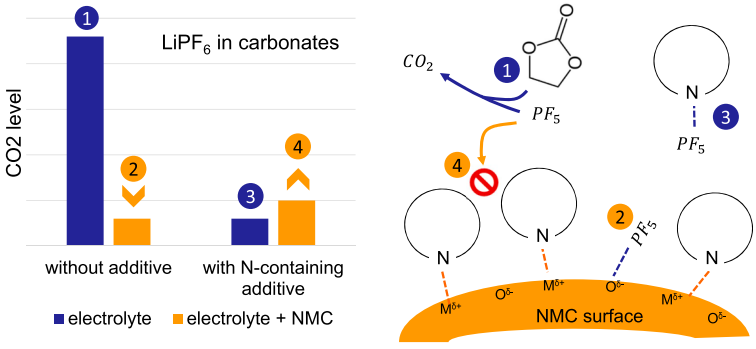

ARTICLE INFO

Keywords:
Battery gassing
Electrolyte additive
Gas chromatography
Thermal degradation
NMC
LiFSI

ABSTRACT

One of the weaknesses of the $LiPF_6$-based electrolyte is its poor thermal stability. It can result in an accelerated battery capacity fading and CO_2 gas generation due to the formation of PF_5 which are highly reactive towards the electrolyte solvents. As the formation of PF_5 is inevitable, efforts are dedicated to inhibiting its deleterious impact by adding a Lewis base to form a complex. However, no study investigates the PF_5-complexation efficiency through gas analysis. Here, gas analysis shows that N-containing additives are effective in reducing gas generation upon electrolyte storage at 55 °C. Out of our expectations, the trend is reversed when it comes to thermal storage of NMC-graphite batteries, involving competitive chemisorption processes on the NMC acid and basic sites. It turned out that, NMC surface can be more effective than additives in mitigating the thermal degradation of the electrolyte. Furthermore, the gas level thermally generated does not decrease while replacing the culprit $LiPF_6$ salt by mixtures of LiFSI + $LiPF_6$ or LiFSI + LiODFB. Especially in presence of LiODFB, water triggers hydrolysis reactions that also lead to gas evolution.

* Corresponding author. Laboratoire de Réactivité et Chimie des Solides, CNRS, UMR 7314, Université de Picardie Jules Verne, 33 rue Saint Leu, 80039, Amiens, France.
E-mail address: stephane.laruelle@u-picardie.fr (S. Laruelle).

https://doi.org/10.1016/j.jpowsour.2024.234901
Received 25 April 2024; Received in revised form 6 June 2024; Accepted 12 June 2024
Available online 16 June 2024

1. Introduction

Commercial lithium-ion batteries often contain an electrolyte composed of [1] a cyclic (ethylene (EC), sometimes with propylene (PC)) and linear (dimethyl (DMC), diethyl (DEC), ethyl methyl (EMC)) carbonate solvents blend, the lithium hexafluorophosphate ($LiPF_6$) salt sometimes mixed with lithium bis (trifluoromethanesulfonyl)imide (LiFSI), and several additives (protective electrode/electrolyte film reinforcement, proton scavengers, flame retardants, etc.) [2]. This electrolyte has long been taken for granted by virtue of its reasonable electrochemical characteristics over a wide range of battery operating temperatures:

- an ionic transport facilitated by i) the dissociation of the salt favored by the high dielectric constant of EC leading to a high ionic conductivity, ii) the ability of the cation to be desolvated in a liquid medium, thus preventing exfoliation of the graphite,
- a wide electrochemical stability window (0–4.3V) owing to the formation of i) an effective passivation layer (AlF_3) on the positive electrode collector surface to prevent aluminum corrosion, thanks to the presence of $LiPF_6$ [3], ii) a passivating layer called solid electrolyte interphase (SEI), on the negative electrode material surface to protect against prolonged carbonate solvent reduction reactions. However, it does not prevent the formation of gas during aging for commercial batteries [4–6].

One of the weaknesses of the $LiPF_6$-based electrolyte is its poor thermal stability. In the literature, the thermally-driven chemical degradation is frequently studied and observed at elevated temperatures as high as 85 °C [7–11], but reactions start well below (<40 °C), obviously in a moderate way [12,13]. This degradation stems from the decomposition of the $LiPF_6$ salt producing PF_5 gas according to reaction (E1). Note that the presence of protons can also generate PF_5 [14], according to reaction (E2). This Lewis acid PF_5 (PF_5>BF_3>HF) [15] is likely to react with trace of water in batteries releasing POF_3 according to reaction (E3).

$$LiPF_{6(sol)} \rightarrow LiF_{(s)} + PF_{5(g)} \quad \text{(E1)}$$

$$PF_{6(sol)}^{-} + H_{(sol)}^{+} \rightarrow PF_{5(g)} + HF_{(sol)} \quad \text{(E2)}$$

$$PF_{5(g)} + H_2O_{(sol)} \rightarrow POF_{3(g)} + 2HF_{(sol)} \quad \text{(E3)}$$

Both PF_5 and POF_3 gases are highly reactive towards the electrolyte solvents. POF_3 reacts directly with cyclic [11] or linear [10] carbonates giving fluorophosphates and CO_2, while PF_5 acts as a catalyst of linear carbonates transesterification reactions or of cyclic carbonates ring-opening polymerization [9] to form ether carbonate oligomers; both processes ending in a decarboxylation process releasing CO_2 gas [8]. We can therefore consider that CO_2 is a good marker of the thermal degradation during battery storage.

Furthermore, PF_5 is likely to react with the basic components of the SEI present on the negative electrode material and with the surface species of the CEI (cathode electrolyte interphase) on the positive electrode material, causing further electrolyte degradation [16] and a loss of Li^+ inventory. These reactions modify the interphase layers composition [17] and yield CO_2 gas release [18]. These temperature-driven reactions can be associated with the HF-induced dissolution of transition metals from cathode materials [19–21], resulting in an accelerated battery capacity fading. E.V. Thomas et al. [22] thus observed a loss of 40 % of the available power and energy for a 18650 lithium-ion cell, after storage at only 50 °C and 100 % SOC for 3 months.

As the formation of PF_5 is inevitable with increasing temperature, a great deal of effort has been dedicated to inhibit its deleterious impact on electrolyte solvents and interphase layers by adding a Lewis base to form a complex. Various bases have been proposed in the literature. A non-exhaustive list is presented in Table 1 (only articles mentioning the formation of a complex with PF_5 were retained).

Typically, three methods are implemented to prove directly or indirectly the formation of a complex between PF_5 and the chosen molecules:

i) **A visual inspection.** In the literature, some PF_5-complexing additives were reported to prevent the electrolyte from turning brown when stored at elevated temperatures [10,23–26], this color being associated with the electrolyte degradation. However, color inspection is insufficient in our opinion as an absence of coloring does not mean an absence of degradation.

ii) **A fluorine or phosphorus NMR analysis.** The formation of three different difluorophosphate or difluorophosphoric acids is detected

Table 1
PF_5-complexing molecules - only articles mentioning a complex with PF_5 are presented here.

Molecule	Ref	Proof of complexation	Improvement of the capacity retention at elevated temperature	Modifying SEI/CEI composition
Tris(2,2,2-trifluoroethyl) phosphite (TFEPi)	[24]	Visual inspection	Not tested	SEI
Trimethyl phosphite (TMPi)	[27]	Sn–Ni anode XPS analysis – less LiF	Not tested	SEI
Hexamethoxycyclo-triphosphazene (HMOPA)	[10, 26]	^{19}F NMR ^{31}P NMR Visual inspection	$LiNi_{0.8}Co_{0.2}O_2$/Gr cell No improvement of charge/discharge capacity after storage for 7 days at 85 °C with 3 wt% of HMOPA.	Not studied
Hexakis(2,2,2-trifluoroethoxy)cyclo-triphosphazene (HFEPN)	[28]	^{19}F NMR $LiN_{0.5}M_{1.5}O_4$ XPS analysis – less LiF	$LiN_{0.5}M_{1.5}O_4$/Li cell After 100 cycles at 60 °C, the capacity retention with 5 wt% HFEPN is 83 %, instead of 58 %	SEI CEI
8-Hydroxyquinoline (8-HDQN)	[23]	Visual inspection $LiN_{0.5}M_{1.5}O_4$ XPS analysis less LiF	$LiN_{0.5}M_{1.5}O_4$/Li cell After 100 cycles at 55 °C, the capacity retention with 0.02 wt% 8-HDQN is 93 %, instead of 61 %	CEI
Pyridine	[26]	^{19}F NMR ^{31}P NMR	Not tested	Not studied
Hexamethyl-phosphoramide (HMPA)	[30]	^{19}F NMR ^{31}P NMR	Not tested	Not studied
Dimethylacetamide	[29]	^{19}F NMR Graphite and $LiFePO_4$ XPS analysis – less LiF	$LiFePO_4$/Gr After 50 cycles at 55 °C, the capacity retention with 1 wt% dimethylacetamide is 87 % instead of 55 %	No reduction or oxidation observed for dimethylacetamide
p-Toluenesulfonyl Isocyanate (PTSI)	[31]	$LiN_{0.5}M_{1.5}O_4$ XPS analysis – less LiF	Not tested	CEI
Diphenyldimethoxysilane (DPDMS)	[25]	Visual inspection $LiNi_{0.6}Mn_{0.2}Co_{0.2}O_2$ XPS analysis – less LiF & presence of Si–F bond	$LiNi_{0.6}Mn_{0.2}Co_{0.2}O_2$/Li cell After 200 cycles at 55 °C, the capacity retention with 1 wt% DPDMS is 93 % instead of 72 %	No reduction or oxidation observed for DPDMS

in degraded electrolytes through ^{19}F and ^{31}P NMR analysis [11]. In case of successful complexation, a set of small peaks emerge along with the strong septet of PF_6 in the ^{31}P NMR spectra and new sets of doublets emerge in ^{19}F NMR spectra corresponding to PF_5 complexes [11]. It is noteworthy that, as with the first method, complex formation is only studied through the electrolyte and not in the complete battery configuration. This aspect will prove to be important in this study.

- **iii) An XPS analysis of the SEI/CEI.** Complex formation prevents PF_5 from reacting with the basic components of the SEI/CEI, thus reducing the amount of LiF visible in the F1s spectra [23,27–29]. The interpretation of the results can be tricky when the additive contains a fluorine atom and has a limited electrochemical stability window. The electrochemical reduction/oxidation of the Lewis-base additive would change the LiF amount of the SEI/CEI.

Surprisingly, no study has investigated the PF_5-complexation efficiency with additives on the thermal stability of the electrolyte through gas analysis. This approach appears to be relevant as it allows the effect of the electrolyte additive to be studied not only from an electrolyte sample as in methods i) and ii), but also from a battery, by sampling the gases and quantifying the CO_2. In addition, a stepwise quantification of the CO_2 released during cycling is supposed to reveal whether the additive is still active or is completely consumed by electrochemical reduction and/or oxidation.

Here, we therefore propose a new approach to studying the effectiveness of additives in complexing PF_5 by quantifying the CO_2 released from both, an electrolyte composed of 1 M $LiPF_6$ in EC/EMC/DEC (1:1:1 vol), and a $LiNi_{1-x-y}Mn_xCo_yO_2$ (NMC)-graphite pouch cell battery prototype. As a highly sensitive device, gas chromatography (GC) coupled with barrier discharge ionization detector (BID) was implemented to provide a rapid and quantitative analysis.

The effectiveness of several additives in reducing gas, proposed in the literature or their derivatives, were first tested in the electrolyte. Those with the best results were then investigated in prototype cells. The second part of the study investigated the effect of replacing the culprit of thermal electrolyte degradation, $LiPF_6$, with mixtures of LiFSI + $LiPF_6$ and LiFSI + lithium difluoro(oxalate)borate (LiODFB) salts.

In particular, this study will show how adsorption phenomena on the active materials can be more effective than additives in mitigating the degradation of the thermal electrolyte, and how residual water can promote gas release in the presence of the LiFSI/LiODFB salt mixture.

2. Experimental

Electrolyte preparation: All electrolytes were prepared in an argon-filled glove box (O_2 and H_2O < 0.1 ppm). The additives (>95 % purity) were added, at a concentration of 0.2 M, in a 1 M $LiPF_6$ in EC/EMC/DEC (1:1:1 vol ratio) commercial electrolyte supplied by Solvionic. Pyridine, 3-methylpyridazine (Me-pyridazine), triethylphosphite (TEPi), (trimethylsilyl)isocyanate (TMSI) and hexamethylphosphoramide (HMPA) were purchased from Sigma Aldrich. Pyrazine, 3-phenylpyridine (Ph-pyridine), 2,6-di-tert-butylpyridine (PyriH), benzo[h]quinoline (BhQ), 3-fluoropyridine (F-pyridine) were purchased from Thermo Scientific, and tris(trimethylsilyl) phosphite (TMSPi) and hexafluorocyclotriphosphazene (HFPN) from TCI. For the evaluation of the lithium salt effect, salt mixtures of LiFSI and $LiPF_6$ (both from Solvionic) or LiODFB (Sigma Aldrich) were dissolved in an EC, EMC and DEC (all from Merck) solvent solution previously prepared in a ratio of 1:1:1 by volume. The water content in all electrolytes was < 10 ppm as determined by Karl Fisher titration (Metrohm KF 756).

Thermal degradation of the electrolyte: To test the effectiveness of the additives on gas generation, in the argon-filled glove box, 173 μL of electrolyte (with or without a 0.2 M additive) was injected into a type 18650 steel can (13.2 mL), covered with a skirted cap tightened by two collars. The impact of the presence of various materials in the electrolyte, namely conductive carbon C45, graphite (GHDR 15-4) (both provided from Imerys) and single crystal $LiNi_{0.8}Mn_{0.1}Co_{0.1}$ (positive active material called NMC811, Umicore), was investigated by placing different amounts of powder (3, 34 and 250 mg, respectively, corresponding to the same surface area of 1350 cm^2) in a 5 mL polypropylene test tube and adding 80 μL of electrolyte (with or without 0.2 M additive). The tubes were covered with a skirt cap tightened with one collar. Cans and tubes were placed in an oven for 24 h at 55 °C before gas recovery. The pKa values of the additives mentioned in the results and discussion section are relative to water as solvent [32]. Although they are different in polar aprotic solvents [33,34], have demonstrated that the pKa order of substituted pyridines and their N-oxides in propylene carbonate solvent is the same as in aqueous solutions.

Thermal degradation of the lithium salts: The thermal degradation of the LiFSI and LiODFB salt mixture was investigated in the absence of carbonate solvents as follows: equimolar amounts of LiFSI and LiODFB powders were intimately mixed in a mortar in the argon-filled glove box. The mixture was then placed in a 5 mL polypropylene test tube sealed with a septum and one collar. Gas analysis was performed after storage at different temperatures for 24 h. Two experiments were carried out, one with the LiODFB powder as received and the other with the LiODFB dried in a Büchi oven at 110 °C for 24 h in the dry room. Amounts of 590 ppm and 5 ppm of water were detected by Karl Fisher titration in the salt mixture, respectively.

Cyclic voltammetry (CV) measurements: Swagelok-type half-cells were assembled in the argon-filled glove box using a 21 μm thick aluminum foil as working electrode, a Whatman GF/C glass fiber separator impregnated with 100 μL of electrolyte, and a lithium metal foil (Sigma Aldrich). CV measurements were conducted on a VMP-3 potentiostat/galvanostat (Biologic), in the 3–6 V range, at a scan rate of 10 mV s^{-1}.

Pouch cells fabrication and cycling: Both single side-coated positive and negative electrodes were laboratory-made under ambient air. The positive electrode was composed of NMC811, carbon black C45 and PVdF binder (Sigma Aldrich) in a 90/5/5 wt ratio. The negative electrode was composed of graphite, C45, CMC, SBR, and Triton-X100 (Sigma Aldrich) in a 93.2/3/2.5/1/0.3 wt ratio. The loading was 14 mg cm^{-2} and 10 mg cm^{-2} of active material, respectively. The final electrodes were calendered to obtain 30–35 % porosity. In the dry room, electrodes of 4 cm^2 and 5.3 cm^2, respectively, were cut and assembled in a pouch cell with a porous polypropylene separator (Celgard 2500). The pouch cell contains a gas pocket of 0.65 mL for gas recovery. They were vacuum-dried overnight at 85 °C before being filled with 80 μL of electrolyte and sealed under vacuum. As determined by Karl Fisher, cells contained 2.9 ± 0.5 μmol of water before electrolyte filling.

Before each experiment, cells were rested for 5 h. Afterwards, they were stored in the oven at 55 °C for 96 h at pristine or charged state after 2 cycles and a charge at C/10 at 25 °C between 2.8 and 4.3 V, with a resting time of 10 min between charge and discharge. Cycling tests were conducted on a VMP 3 potentiostat/galvanostat (Biologic).

Gas Analysis: 0.5 mL gas is extracted using a syringe and injected (injection mode – direct) into a gas chromatograph (GC-2010 from Shimadzu corporation) combined with barrier ionization detector (BID). The carrier gas is helium and the used GC column is a packed column 1010 PLOT Capillary 30 m × 0.53 mm from Carboxen. Measurements were performed at 100 °C with a pressure of 26 kPa (flow control mode – pressure). To quantify, CO_2 and CO, a calibration mixture gas was used. The error of each value was determined from 3 measurements, and corresponds to the difference between the minimum and maximum value.

3. Results & discussions

3.1. Screening of additives

Based on the literature, several additives have been tested in this work for their efficiency in trapping PF_5 without even considering their

electrochemical stability window. For this purpose, an EC/EMC/DEC (1:1:1 wt%) 1 M $LiPF_6$ electrolyte formulated without or with 0.2 M additives was stored in a stainless steel can for 24 h at 55 °C. The released gas was analyzed and only CO_2 was detected and quantified by GC-BID (Fig. S1a). We also carried out these experiments for 96 h and an additional trace of CO was found (Fig. S1b). We assume that the CO comes from additional degradation of products but no mechanisms have been proposed to date. As shown in Fig. 1, these additives feature different efficiencies in reducing the amount of CO_2, in the following order; pyridine > TMSI > HMPA > HFPN. On the other hand, the additives, TEPi and TMSPi lead to the same CO_2 level evolution than the control electrolyte without additive, thus demonstrating that they are not active in complexing PF_5 and thus in reducing thermal decomposition of carbonate solvents into CO_2.

It is worth pointing out here that some additional studies, Fig. S2 in the SI section, focusing on the kinetic of electrolyte decomposition during storage, in presence of different additive concentrations, have shown that, under these conditions, PF_5 can catalyze the decomposition of around five solvent molecules.

To inhibit this degradation, PF_5 complexation with a Lewis base containing atoms with lone-pair electrons is required. Therefore, all the tested nitrogen-containing molecules were candidate additives to form complexes. The fact that the lone-pair electrons of nitrogen in pyridine are not delocalized in the π aromatic system but in sp^2 orbital endows this molecule with basic properties enabling to play an active role in the PF_5 complexation. As for TMSI and HMPA additives, despite the fact that the lone-pair electrons of the nitrogen are delocalized with those of the oxygen from the electron-withdrawing C=O or P=O adjacent groups, the basicity of the molecules is sufficient to attenuate the PF_5 reactivity toward carbonate solvents but to a lesser extent than pyridine. On the other hand, it should be noted that the CO_2 amount does not decrease significantly with the addition of hexafluorocyclotriphosphazene (HFPN). The class of phosphazene was tested by Campion et al. [10] and Kim et al. [28] with the following molecules, hexamethoxycyclotriphosphazene (HMOPA) and hexakis(2,2,2-trifluoroethoxy) cyclo-triphosphazene (HFEPN), containing OCH_3 and OCH_2CF_3 groups, respectively, in place of fluorine atoms. HMOPA was found to inhibit the electrolyte thermal degradation until 2000 h of storage at 85 °C while in Ref. [28], it is assured that HFEPN can also form complex with PF_5, although their NMR study only examined the ability of the additive to trap HF or block the $LiPF_6$ hydrolysis. In both cases, no gas studies have been undertaken, which makes it difficult to compare the efficiency of HMOPA and HFEPN with that of HFPN. The inefficiency of HFPN observed in our study can be explained by the presence of electron-withdrawing fluorine atoms attached to phosphorus, making the molecule too much acidic.

Finally, Fig. 1 does not reveal any decrease in the CO_2 amount with the addition of phosphite molecules (TEPi and TMSPi), although, as reported in Table 1, some authors [24,27] suggested that they complex with PF_5 from visual inspection or XPS analysis. Indeed, S. S. Zhang et al. [24] did not observe electrolyte coloration with tris(2,2,2-trifluoroethyl) phosphite (TFEPi) and M. H. Choo et al. [27] observed less LiF in the SEI with trimethylphosphite (TMPi). If these molecules, TMPi and TFEPi, are expected to stabilize PF_5, then TEPi tested in this work, with a higher electron donor group, (CH_3CH_2O (TEPi) > CH_3O(TMPi) > OCH_2CF_3(TFEPi)) should be more likely to cause complexation. As no effect is observed with TEPi (Fig. 1), it can be assumed that TMPi and TFEPi should have no effect on reducing CO_2 release either.

On the other hand, the chemical reactivity of the TMSPi additive has been the subject of several studies [35,36]. Most of the papers reported the presence of $FSi(Me)_3$ as a degradation product. In Ref. [35], the authors hypothesized that the lone pair electrons of phosphorus in the phosphite molecule allowed coordination of PF_5; the complex would decompose, leading to the formation of $FSi(Me)_3$. However, the latter was also reported by the same authors to be one of the decomposition products of the rapid reaction between TMSPi and the anion PF_6^-. Our results tend to show that TMSPi does not complex nor generate PF_5 upon the reaction between TMSPi and PF_6^-. Moreover, TMSPi has been more widely reported in the literature to trap HF [37,38], thereby reducing the dissolution of transition metals from the positive active material surface.

In summary, although all molecules tested, selected from the literature review, were expected to scavenge PF_5, analysis of the CO_2 levels released during electrolyte storage at high temperature shows that only the nitrogen-containing additives are effective in inhibiting solvent degradation. As pyridine exhibited the highest efficiency among the different families of molecules, six other single-N-containing heterocyclic compounds were investigated as a function of their basicity, namely 3-phenylpyridine (Ph-pyridine), benzo[h]quinoline (BhQ), 2,6-di-tert-butylpyridine (PyriH) and 3-fluoropyridine (F-pyridine), and two 2-N-containing heterocycles namely, 3-methylpyridazine (Me-pyridazine) and pyrazine.

3.2. *Assessment of N-containing heterocyclic additives as a function of their basicity*

A legitimate question arose concerning the basicity of the molecules, i.e. to which minimum pKa value they have sufficient electron donating ability to form an adduct with PF_5. As an attempt to answer this question, the effectiveness of various N-containing heterocyclic additives featuring lower pKa (4.8 down to 0.6) than pyridine (5.2) was examined after storage of the electrolytes at 55 °C for 24 h. As shown in Fig. 2, the additives, Ph-pyridine (pKa = 4.8), BhQ (pKa = 4.2), F-pyridine (pKa = 3.1) and Me-pyridazine (pKa = 2.8) play a beneficial effect similar to pyridine, with CO_2 amount values inferior to 10 µmol. Note that the

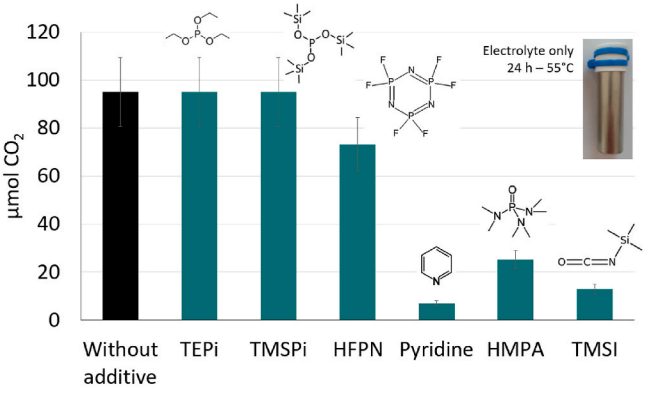

Fig. 1. Quantity of CO_2 recovered from an 18650 can containing an electrolyte without and with 0.2 M additive after 24 h storage at 55 °C.

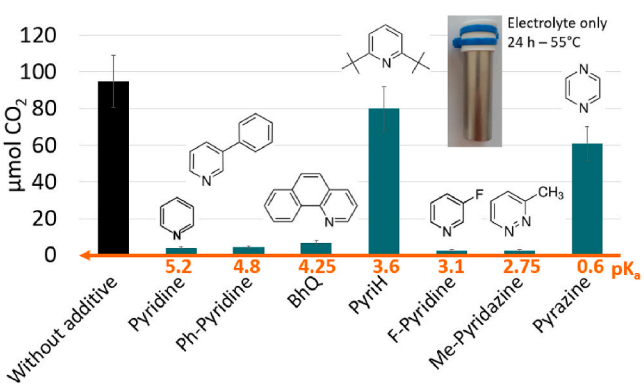

Fig. 2. CO_2 release from electrolyte stored in an 18650 can heated to 55 °C for 24 h, without (black) or with 0.2 M additive.

additive BhQ is slightly less effective (7.0 ± 1 compared with 4.4 ± 1 μmol for pyridine) which could be explained by the steric hindrance due to the benzene group almost facing nitrogen. On the other hand, the PyriH (pKa = 3.6) additive does not result in a tangible decrease in the CO_2 level (80 ± 12 μmol) compared to the control electrolyte (95 ± 15 μmol). This result was expected from this hindered base, as the accessibility of the nitrogen lone pair electrons for PF_5 complexation is significantly limited owing to the large steric effect of the bulky *tert*-butyl groups.

Among the additives tested, Me-pyridazine (pKa = 2.8) and pyrazine (pKa = 0.6) display the lowest pKa values. As far as the pyrazine is concerned, the addition of a second nitrogen atom induces a delocalization of the pair of non-bonding electrons into the aromatic ring due to π-σ bond alternation [39] which notably decreases the basicity properties of the molecule. As a result, pyrazine is less effective in complexing PF_5 as revealed by the relatively high amount of CO_2 (61 ± 10 μmol). This π-σ bond alternation does not take place in the case of the Me-pyridazine molecule in which the two nitrogen atoms are adjacent. The lone pair electrons can repulse each other but have sufficient donor ability to complex PF_5, resulting in a significant CO_2 level decrease.

Overall, this study demonstrates that N-containing heterocyclic additives could play an important role in scavenging PF_5 during high temperature storage of a classical Li-ion electrolyte. In view of these interesting results, we undertook a quantitative investigation of the role of these additives on the CO_2 evolution within a NMC/graphite pouch cell prototype.

3.3. Assessment of the selected additives in NMC/graphite pouch cell prototype

NMC811/graphite pouch cells were filled with a 0.2 M additive-containing electrolyte, then the amount of produced CO_2 was quantified after storage at 55 °C for 96 h (Fig. 3a) without any prior cycling step that might have led to electrochemical reduction or oxidation of the additive. Note that, trace of CO was also detected as in previous 18650 can tests after 96 h of storage (see Fig. S1d). Overall, all values are much lower than the ones obtained from cans (Figs. 1 and 2). This is explained by a smaller dead volume (0.65 mL in pouch cell against 13.2 mL in steel can), which limit the generation of PF_5 gas, as further shown in Fig. S3 in the SI section. More importantly, all the CO_2 levels obtained with the additive-containing electrolytes were higher than those obtained with the control electrolyte, in stark contrast to the results reported above for electrolytes stored in cans. Furthermore, the more acidic the additives, the higher the CO_2 levels, as revealed by the different N-containing heterocyclic additives (from approx. 0.2 to 1.2 μmol for additives with pKa from 5.2 to 2.8, respectively). Intrigued by these findings, we wanted to find out more about the exact role played by the materials in contact with the electrolyte.

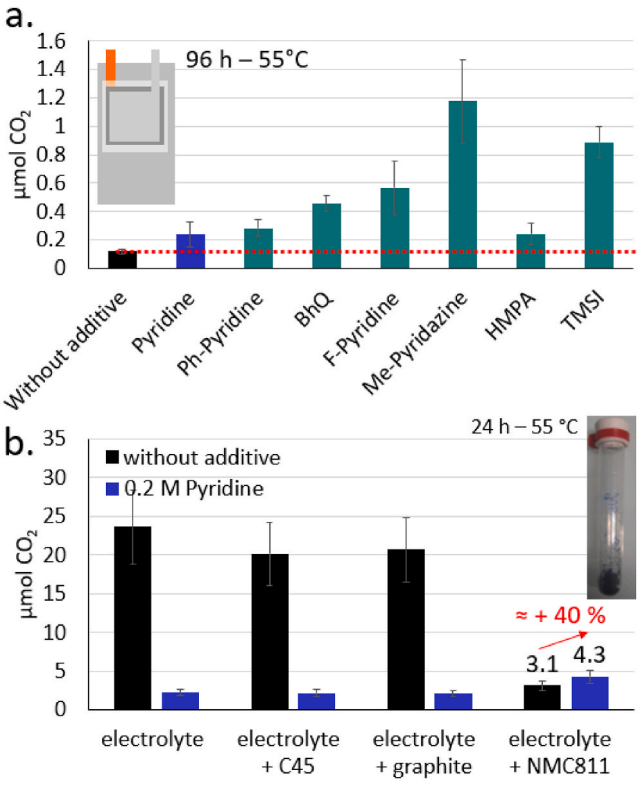

Fig. 3. a) CO_2 quantity produced from 0.2 M additive electrolyte impregnated in an assembled NMC811/graphite pouch cell prototype, after storage at 55 °C for 96 h. b) CO_2 quantity produced from electrode material (same surface area)/electrolyte stored at 55 °C for 24 h in a polypropylene tube.

We therefore stored the different electrode materials (same surface area), namely the conductive carbon C45, graphite and NMC811 powders, separately, impregnated in an electrolyte solution with and without pyridine, the most efficient additive (Fig. 3b), at 55 °C for 24 h in polypropylene tube.

In the absence of pyridine, the carbonaceous powders, C45 and graphite have a very small impact (-ca. 12 %) on the CO_2 level decrease as compared to the NMC811 material (-ca. 87 %). This trend was also observed for other grades of NMC (Fig. S4) with however a most significant drop in CO_2 level, as the nickel content increases (-ca. 83 % and 91 % for NMC containing 60 % and 90 % of Ni respectively). These outcomes clearly demonstrate that the cathode material could play a significant role in mitigating electrolyte degradation. This was also observed by Campion et al. [10] at 85 °C with $LiCo_xNi_{1-x}O_2$ and $LiCoO_2$ powders at the discharged (or charged) state by a visual inspection. We can assume that most of the PF_5 formed upon storage at elevated temperature are deactivated through chemisorption onto the basic sites of the lamellar oxide (O^{2-}) (path 2), as illustrated in Fig. 4a. Indeed, in the field of catalysis, it is known that the surface of oxides offers acid-base properties attributed to the cations ($M^{+\delta}$) and anions (O^{2-}), respectively [40,41]. In our experiment, the basic properties of the O^{2-} anions at the surface of the cathode material are apparently strong enough to share electrons with the PF_5 adsorbates. It should be noted that basic surface species (Li_2CO_3 and Li_2O) can be present at the surface of Ni-rich lamellar oxides (Ni > 0.5 in $LiNi_{1-x-y}Mn_xCo_yO_2$) [18,42], so a prior reaction of PF_5 with these compounds is likely to take place to give PF_5 access to the basic sites.

As expected, a striking decrease in CO_2 level is observed by adding 0.2 M pyridine in control electrolyte or in the carbonaceous material-added electrolytes (from ca. 20–24 μmol without additive to ca. 2 μmol with pyridine, i.e. −90 %). This clearly demonstrates the role of the additive in inhibiting solvent degradation through PF_5 scavenging. However, in case of NMC-added electrolyte, the CO_2 level is increased by ca. 40 % when adding pyridine (from 3.1 to 4.3 μmol). And the higher the concentration of pyridine, the greater the CO_2 level (Fig. S5). This result is surprising at first sight, since we expected a cumulated effect of the PF_5-scavenging role of both the basic additive and the basic anion (O^{2-}) sites of the NMC surface. Considering the above, it was assumed that pyridine could first chemisorb onto the acid cation ($M^{+\delta}$) sites [43] on the surface of the NMC particles, thereby limiting the adsorption of PF_5 on the basic anion (O^{2-}) sites (path 2) upon storage, as illustrated in Fig. 4b. In this case, PF_5 could also be scavenged by remaining basic additive molecules in the electrolyte (path 3) or react with solvent (path 1) to a slightly greater extent as revealed by the CO_2 level increase.

As shown in Fig. 3a, similar phenomena involving chemisorption of the additive on the acid sites of the NMC surface, thus preventing chemisorption trapping of PF_5, may occur in the cells, explaining the higher level of CO_2 in the presence of additives. The presence of less basic molecules than pyridine leads to even higher production of CO_2. This may be a result of the reduced ability of the residual part of

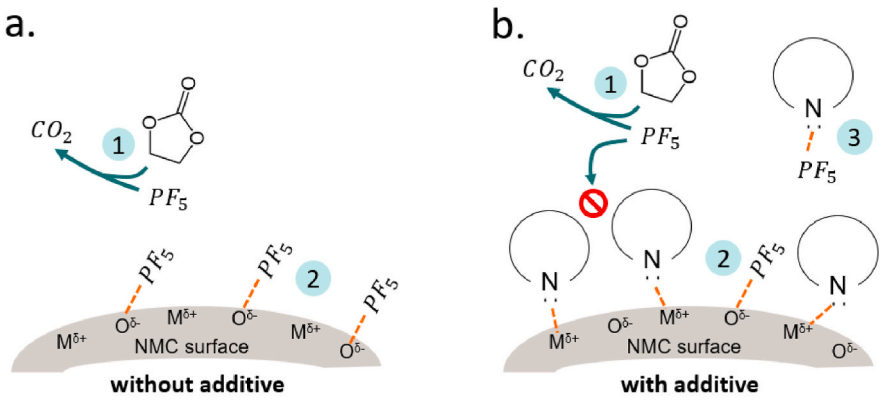

Fig. 4. Illustration of the different paths of PF_5 reactivity during storage of NMC material impregnated in a) a control electrolyte b) a Lewis base additive-added electrolyte. Path 1: PF_5 as a catalyst of solvent degradation. Path 2: adsorption of PF_5 on NMC basic anion (O^{2-}) sites. Path 3: complexation of PF_5 with Lewis base additive.

additives located in other parts of the pouch cell to trap PF_5 in electrolyte.

All these results demonstrate the effectiveness of NMC in combating the thermal degradation of the $LiPF_6$-based carbonate electrolyte and the counterproductive effect of adding basic additives.

3.4. Impact of replacing $LiPF_6$ by LiFSI salt

Assessing the impact of the replacement of $LiPF_6$ by LiFSI appeared as an alternative solution to inhibit the electrolyte thermal degradation upon storage of NMC containing pouch cells. As preliminary investigations, both $LiPF_6$- and LiFSI-based carbonate electrolytes were tested upon storage in an 18650 can at 55 °C for 24 h. As anticipated (Fig. 5a), the amount of CO_2 released by the LiFSI electrolyte is very low compared with that released by the $LiPF_6$ electrolyte (ca. 0.6 µmol *vs.* ca. 95 µmol, resp.). However, cells impregnated with an electrolyte based solely on LiFSI salt are known to suffer from electrochemical instability during charging due to corrosion of the aluminum collector [3]. As an already literature-proposed solution to overcome this problem is the use of mixtures of LiFSI with other passivating salts, $LiPF_6$ [3] or LiODFB [44], we embarked first into an aluminum corrosion study to select the best ratio. As shown in Fig. 6, voltammograms depict very low characteristic anodic current in the case of the blends 0.7 M LiFSI + 0.3 M $LiPF_6$ and 0.8 M LiFSI + 0.2 M LiODFB as compared to the case of LiFSI (1 M) electrolyte. LiODFB would be slightly more effective at protecting the aluminum collector than $LiPF_6$. As these electrolytes prevent continuous corrosion up to 6V against Li/Li^+, they were selected to assess thermal degradation in can and pouch cell by quantifying CO_2 and CO gas.

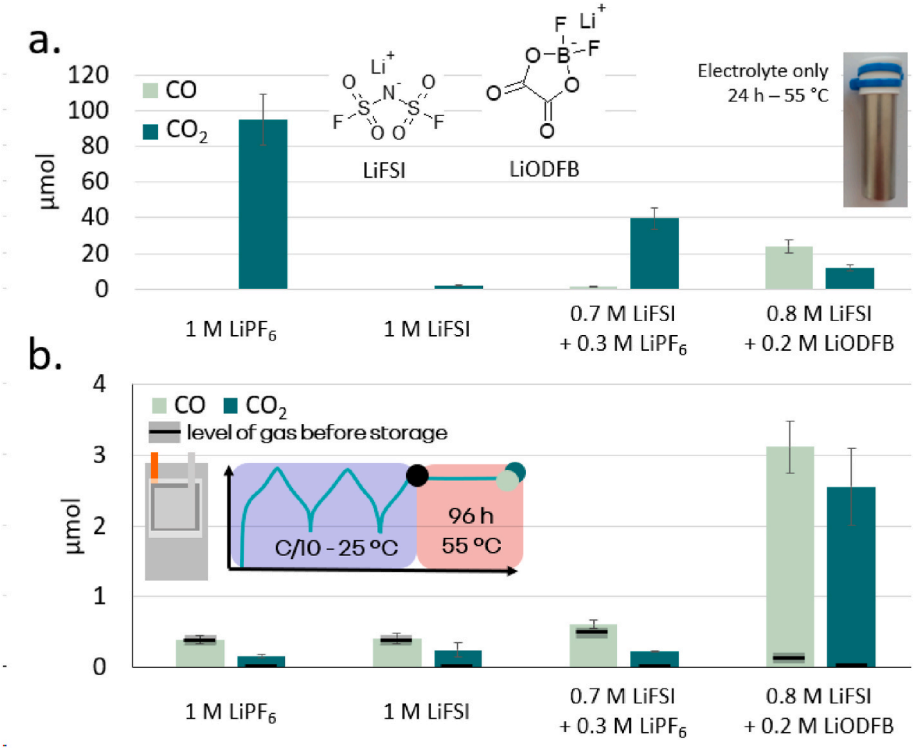

Fig. 5. CO_2 and CO level produced from a) 18650 cans after storage at 55 °C for 24 h of electrolytes containing different salts or salt mixtures in carbonate solvents b) 0.2 M additive electrolyte impregnated in an assembled NMC811/graphite pouch cell prototype, after 5 h impregnation, formation cycles (2 cycles and a charge at C/10 at 25 °C) and storage or not at 55 °C for 96 h.

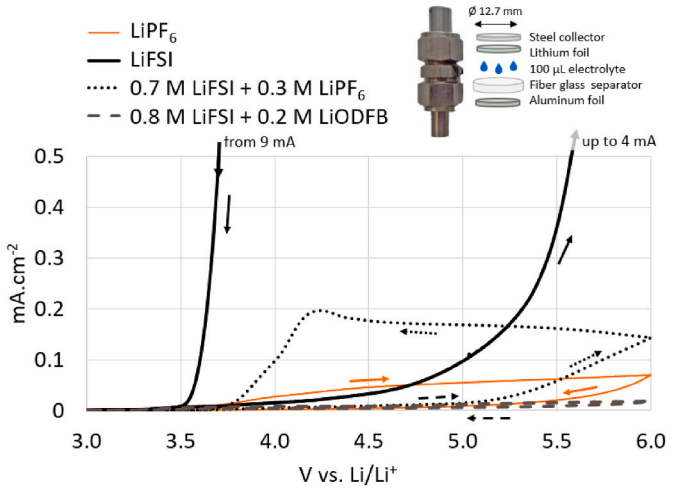

Fig. 6. Cyclic voltammograms of electrolyte containing 1 M LiFSI, 1 M $LiPF_6$, 0.7 M LiFSI + 0.3 M $LiPF_6$, and 0.8 M LiFSI + 0.2 M LiODFB.

When stored in cans, the 0.7 M LiFSI + 0.3 M $LiPF_6$ electrolyte releases less CO_2, i.e. only ca. 42 % of the amount released from $LiPF_6$ (1 M) electrolyte. On the other hand, the 0.8 M LiFSI + 0.2 M LiODFB electrolyte releases CO_2 (12.6 %) and even more CO. Obviously, being an oxalate salt, LiODFB was initially accused of being the source of these gases. However, LiODFB (1 M) electrolyte tested under similar conditions did not show any gas release. As the presence of both salts seemed to be essential to produce CO_2 and CO, we first tried to find out more about the origin of these gases, whether they came from the carbonate solvents or from the LiODFB salt itself. To do so, an equimolar amount of salt powders was mixed in a mortar inside the glovebox prior to being introduced into a plastic tube. Suspecting that water was involved in the degradation mechanisms, two storage experiments were carried out, one with LiODFB salt as received, the other with dried salt. As shown in Table 2, CO and CO_2 were produced in fairly equivalent proportions in the two experiments, hinting that LiODFB was the source of the gas released during electrolyte storage and not the solvents. Besides, it can be noticed that the quantities of CO and CO_2 are in the same range as that of water detected by Karl Fisher analysis. On the basis of the above data, the subsequent degradation reaction pathways can be proposed, starting with the hydrolysis of LiFSI. Zhou et al. [45] proposed that, under neutral conditions, with low water content, the following reaction (E4) happens:

$$2\ N(FSO_2)_2^- + 4H_2O \rightarrow FSO_2NH_2 + NH_2SO_3^- + FSO_3^- + SO_4^{2-} + 2HF + 2H^+ \quad (E4)$$

An electrophilic attack of the protons on LiODFB following reaction (E5) would occur to yield equimolar amount of CO and CO_2:

$$LiF_2BC_2O_4 + H^+/HF \rightarrow BF_2OH + CO + CO_2 + Li^+/LiF \quad (E5)$$

As a less electron attractor than BF_3, the question of the reactivity of the Lewis acid, BF_2OH, still arises as to whether it can simply complex EC or also activate its degradation; a concern that would require more in-depth investigation.

In order to assess the role of temperature in activating such water-initiated degradation processes, additional powder storage tests were carried out with the 0.5 M LiFSI + 0.5 M LiODFB salt mixture at 25, 35 and 45 °C for 24 h. As can be seen in Table 2, the amounts of CO and CO_2 are non-existent to very low from 25 to 45 °C, then increase abruptly at 55 °C. This release of gas was accompanied with a change in color of the whole tube towards pink. This is consistent with results reported in the literature, where it has been clearly shown that hydrolysis of LiFSI does not occur at 30 °C [46] and accelerates with increasing temperature when studied from 65 to 85 °C [45]. In Ref. [45], similar color change into rosiness was observed upon LiFSI degradation.

This unveils another deleterious impact that the ever-present water can have on the functioning of cells. The protons produced by the thermally driven hydrolysis of LiFSI can lead to LiODFB decomposition during storage, even before it can play its role as an SEI (or CEI) reinforcing additive [47,48] or a passivating agent against aluminum corrosion [49].

The four electrolytes formulated with 1 M $LiPF_6$, 1 M LiFSI, 0.7 M LiFSI + 0.3 M $LiPF_6$ and 0.8 M LiFSI + 0.2 M LiODFB were then impregnated in pouch cells prototype. These cells were subjected to a formation cycling step at 25 °C then gas analysis was carried out before and after storage at 55 °C for 96 h. Consistent with the absence of thermal degradation at 25 °C, it can be noticed before storage the quasi-absence of CO_2 (Fig. 5b – black bars). Quantities around 0.5 ± 0.1 µmol of CO are released from the first three electrolytes while only 0.2 ± 0.07 µmol of CO are released from the fourth one. The production of CO is known to come from the electrochemical reduction of the solvents [50]. It can therefore be concluded that the reduction of LiODFB [49] occurring at high potential (around 1.5V vs. Li/Li^+) creates a SEI that limits the reduction of carbonates (around 0.8 V vs. Li/Li^+).

After formation and storage steps, CO_2 levels slightly increases (<0.4 µmol) in case of the first three electrolytes. In agreement with the above results, $LiPF_6$-based electrolytes produce little CO_2 due to chemisorption of PF_5 on the acid sites of lamellar oxides and LiFSI-based electrolytes do not produce solvent degradation catalysts. In contrast, cells with the fourth 0.8 M LiFSI + 0.2 M LiODFB electrolyte release high amounts of CO (3.1 ± 0.4 µmol) and CO_2 (2.6 ± 0.6 µmol). As observed in salt mixture powder tests (Table 2), these quantities are in the same range as that of water detected by Karl Fisher analysis; 2.4 ± 0.3 µmol of water have been detected in cells without electrolyte after 24 h vacuum-drying at 85 °C (this value corresponds to 230 ± 30 ppm of water considering the free-electrolyte cell and 470 ± 55 ppm of water considering only the electrolyte). This result highlights, according to the above-mentioned proposed reaction paths (E4-E5), the role of water in cells on LiFSI hydrolysis and consequently on LiODFB degradation.

To conclude, replacing $LiPF_6$ by LiFSI does not mitigate the thermal degradation of electrolyte solvents in NMC-based cells after storage at 55 °C for 96 h. However, the use of LiFSI brings beneficial properties such as improved conductivity [46,51], better capacity retention when used as lithium salt [52] or additive [53], and lower impedance (thinner SEI with higher content of LiF) [53].

Table 2
amount of CO and CO_2 after storage for 24 h of 0.2 g of LiFSI/LiODFB salt mixture (1:1 mol) in a closed polypropylene tube.

Water content (µmol H_2O)	Wet 6.5 ± 0.4				Dry 0.05 ± 0.01
Storage temperature (°C)	25	35	45	55	55
CO - µmol	0	0	0.010 ± 0.002	3.9 ± 0.7	0.020 ± 0.002
CO_2 - µmol	0.05 ± 0.03	0.11 ± 0.03	0.43 ± 0.06	4.3 ± 0.7	0.33 ± 0.03

4. Conclusion

The quantitative analysis of CO_2 released from the thermal storage of electrolyte samples or pouch cell prototypes proved to be relevant for investigating the different measures to counteract the degradation of the $LiPF_6$-based electrolyte.

As anticipated, the presence of a Lewis base additive in electrolyte reduces the gas formation during its storage at 55 °C and its efficiency through PF_5-complexing is consistent with its acid-base property. However, when the electrolyte is impregnated in NMC/graphite cells, the additive no longer plays its role due to other complexation processes taking place on the NMC surface.

Without additives, PF_5 can chemisorb on the basic sites of NMC, which then acts as an efficient PF_5-complexing agent. However, this process is mitigated when a PF_5 complexing additive is added to the electrolyte. The additive can chemisorb on the acidic sites of the NMC, preventing PF_5 from accessing the basic sites, making them available for the catalysis of solvent decomposition.

In the presence of NMC, replacing $LiPF_6$ with a LiFSI + $LiPF_6$ or LiFSI + LiODFB salt mixture does not further reduce the gas levels. In addition, the water present in the battery triggers the hydrolysis of LiFSI and subsequently the electrophilic attack of protons on LiODFB, releasing CO and CO_2 gas.

This work demonstrates the ability of the NMC to complex PF_5. However, as this study was carried out over a relatively short storage period, not exceeding 96 h, the question arises as to at what stage of battery ageing the active material would be saturated by the PF_5 produced throughout the life of the battery, and no longer be effective. The use of N-based additives may seem a good option, but our tests showed that at a concentration of 0.2 M, they were unable to reduce the production of CO_2 to the level of that without the additive. To be more effective, an increase in its concentration would be required, which could cause harmful effects. Moreover, the complexation reaction with PF_5 is an irreversible process that will consume the additive until it could no longer prevent thermal degradation.

LiFSI-based electrolytes remain the best solution for countering the off-gassing induced by the thermal degradation of the electrolyte. However, its ineffectiveness in completely protecting the aluminum collector from corrosion necessitates the use of a co-salt. LiODFB seems to be a good candidate, but its reactivity in the presence of protons may be a hindrance. It would therefore be interesting in the future to find new co-salts for the use of LiFSI.

CRediT authorship contribution statement

Baptiste Salomez: Writing – original draft, Investigation, Formal analysis, Conceptualization. **Sylvie Grugeon:** Writing – original draft, Investigation, Conceptualization. **Pierre Tran-Van:** Writing – review & editing, Supervision, Conceptualization. **Stephane Laruelle:** Writing – review & editing, Supervision, Conceptualization.

Declaration of competing interest

The authors declare that they have no known competing financial interests or personal relationships that could have appeared to influence the work reported in this paper.

Data availability

Data will be made available on request.

Acknowledgments

The financial support from the Association Nationale de la Recherche et de la Technologie (ANRT, France) is gratefully acknowledged. The authors thank Umicore for NMC cathode materials supply. Michel Armand is thanked for his help and fruitful discussions.

Appendix A. Supplementary data

Supplementary data to this article can be found online at https://doi.org/10.1016/j.jpowsour.2024.234901.

References

[1] N.P. Lebedeva, F.D. Persio, T. Kosmidou, D. Dams, A. Pfrang, A. Kersys, L. Boon-Brett, Amount of free liquid electrolyte in commercial large format prismatic Li-ion battery cells, J. Electrochem. Soc. 166 (4) (2019) A779, https://doi.org/10.1149/2.1151904jes, mars.

[2] S.S. Zhang, A review on electrolyte additives for lithium-ion batteries, J. Power Sources 162 (2) (nov. 2006), https://doi.org/10.1016/j.jpowsour.2006.07.074, 2.

[3] C. Forestier, S. Grugeon, C. Davoisne, A. Lecocq, G. Marlair, M. Armand, L. Sannier, S. Laruelle, Graphite electrode thermal behavior and solid electrolyte interphase investigations: role of state-of-the-art binders, carbonate additives and lithium bis (fluorosulfonyl)imide salt, J. Power Sources 330 (2016) 186–194, https://doi.org/10.1016/j.jpowsour.2016.09.005, oct.

[4] J. Schmitt, Measurement of gas pressure inside large-format prismatic lithium-ion cells during operation and cycle aging, J. Power Sources 10 (2020).

[5] A. Matasso, D. Wong, D. Wetz, F. Liu, Correlation of bulk internal pressure rise and capacity degradation of commercial $LiCoO_2$ cells, J. Electrochem. Soc. 161 (14) (2014) A2031–A2035, https://doi.org/10.1149/2.0221414jes.

[6] A. Matasso, D. Wong, D. Wetz, F. Liu, Effects of high-rate cycling on the bulk internal pressure rise and capacity degradation of commercial LiCoO2 cells, J. Electrochem. Soc. 162 (6) (2015) A885, https://doi.org/10.1149/2.0461506jes, mars.

[7] S.E. Sloop, J.K. Pugh, S. Wang, J.B. Kerr, K. Kinoshita, Chemical reactivity of PF 5 and LiPF6 in ethylene carbonate/dimethyl carbonate solutions, Electrochem. Solid State Lett. 4 (4) (2001) Art, https://doi.org/10.1149/1.1353158, 4, févr.

[8] B. Ravdel, K.M. Abraham, R. Gitzendanner, J. DiCarlo, B. Lucht, C. Campion, Thermal stability of lithium-ion battery electrolytes, J. Power Sources 119–121 (2003) 805–810, https://doi.org/10.1016/S0378-7753(03)00257-X, juin.

[9] S.E. Sloop, J.B. Kerr, K. Kinoshita, The role of Li-ion battery electrolyte reactivity in performance decline and self-discharge, J. Power Sources 119–121 (2003) 330–337, https://doi.org/10.1016/S0378-7753(03)00149-6, juin.

[10] C.L. Campion, W. Li, W.B. Euler, B.L. Lucht, B. Ravdel, J.F. DiCarlo, R. Gitzendanner, K.M. Abraham, Suppression of toxic compounds produced in the decomposition of lithium-ion battery electrolytes, Electrochem. Solid State Lett. 7 (7) (2004) A194, https://doi.org/10.1149/1.1738551.

[11] C.L. Campion, W. Li, B.L. Lucht, Thermal decomposition of LiPF6-based electrolytes for lithium-ion batteries, J. Electrochem. Soc. 152 (2005) A2327, https://doi.org/10.1149/1.2083267.

[12] S. Rigaud, A.C. Martinez, T. Lombard, S. Grugeon, P. Tran-Van, S. Pilard, S. Laruelle, Mass spectrometry analysis of nmc622/graphite Li-ion cells electrolyte degradation products after storage and cycling, J. Electrochem. Soc. 169 (1) (2022), https://doi.org/10.1149/1945-7111/ac44bb, 1, janv.

[13] V. Kraft, W. Weber, M. Grützke, M. Winter, et S. Nowak, « Study of decomposition products by gas chromatography-mass spectrometry and ion chromatography-electrospray ionization-mass spectrometry in thermally decomposed lithium hexafluorophosphate-based lithium ion battery electrolytes, RSC Adv. 5 (98) (sept. 2015) 80150–80157, https://doi.org/10.1039/C5RA16679A.

[14] S. Solchenbach, M. Metzger, M. Egawa, H. Beyer, H.A. Gasteiger, Quantification of PF_5 and POF_3 from side reactions of $LiPF_6$ in Li-ion batteries, J. Electrochem. Soc. 165 (13) (2018), https://doi.org/10.1149/2.0481813jes, 13.

[15] K.O. Christe, D.A. Dixon, D. McLemore, W.W. Wilson, J.A. Sheehy, J.A. Boatz, On a quantitative scale for Lewis acidity and recent progress in polynitrogen chemistry, J. Fluor. Chem. (2000) 3.

[16] H.H. Lee, C.C. Wan, Y.Y. Wang, Thermal stability of the solid electrolyte interface on carbon electrodes of lithium batteries, J. Electrochem. Soc. 151 (4) (2004) A542, https://doi.org/10.1149/1.1647568.

[17] M. Herstedt, D.P. Abraham, J.B. Kerr, K. Edström, X-ray photoelectron spectroscopy of negative electrodes from high-power lithium-ion cells showing various levels of power fade, Electrochim. Acta 49 (28) (nov. 2004), https://doi.org/10.1016/j.electacta.2004.06.021, 28.

[18] A.C. Martinez, S. Grugeon, D. Cailleu, M. Courty, P. Tran-Van, B. Delobel, S. Laruelle, High reactivity of the nickel-rich LiNi1-x-yMnxCoyO2 layered materials surface towards H2O/CO2 atmosphere and LiPF6-based electrolyte, J. Power Sources 468 (2020) 228204, https://doi.org/10.1016/j.jpowsour.2020.228204 août.

[19] D.R. Gallus, R. Schmitz, R. Wagner, B. Hoffmann, S. Nowak, I. Cekic-Laskovic, R. W. Schmitz, et M. Winter, The influence of different conducting salts on the metal dissolution and capacity fading of NCM cathode material, Electrochim. Acta 134 (2014) 393–398, https://doi.org/10.1016/j.electacta.2014.04.091, juill.

[20] W. Li, Review—an unpredictable hazard in lithium-ion batteries from transition metal ions: dissolution from cathodes, deposition on anodes and elimination strategies, J. Electrochem. Soc. 167 (9) (2020), https://doi.org/10.1149/1945-7111/ab847f, 9, avr.

[21] J.L. Tebbe, A.M. Holder, C.B. Musgrave, Mechanisms of LiCoO2 cathode degradation by reaction with HF and protection by thin oxide coatings, ACS Appl. Mater. Interfaces 7 (43) (2015) 24265–24278, https://doi.org/10.1021/acsami.5b07887, nov.

[22] E.V. Thomas, H.L. Case, D.H. Doughty, R.G. Jungst, G. Nagasubramanian, E. P. Roth, Accelerated power degradation of Li-ion cells, J. Power Sources 124 (1) (2003) 254–260, https://doi.org/10.1016/S0378-7753(03)00729-8, oct.

[23] H. Shang, H. Zhou, G. Jingjing, H. Zhang, T. Li, Y. Qiao, W. Niu, M. Qu, Z. Xie, G. Peng, Improving the cyclic stability of LiNi0.5Mn1.5O4 cathode by modifying the interface film with 8-hydroxyquinoline, ChemistrySelect 6 (16) (2021) 3988–3994, https://doi.org/10.1002/slct.202100754.

[24] S.S. Zhang, K. Xu, T.R. Jow, A thermal stabilizer for LiPF6-based electrolytes of Li-ion cells, Electrochem. Solid State Lett. 5 (9) (2002), https://doi.org/10.1149/1.1499669, 9, juill.

[25] B. Deng, H. Wang, W. Ge, X. Li, X. Yan, T. Chen, M. Qu, G. Peng, Investigating the influence of high temperatures on the cycling stability of a LiNi0.6Co0.2Mn0.2O2 cathode using an innovative electrolyte additive, Electrochim. Acta 236 (2017) 61–71, https://doi.org/10.1016/j.electacta.2017.03.155, mai.

[26] W. Li, C. Campion, B.L. Lucht, B. Ravdel, J. DiCarlo, K.M. Abraham, Additives for stabilizing LiPF6-based electrolytes against thermal decomposition, J. Electrochem. Soc. 152 (2005) A1361, https://doi.org/10.1149/1.1926651.
[27] M.-H. Choo, C.C. Nguyen, S. Hong, Y.H. Kwon, S.-W. Woo, J.Y. Kim, S.-W. Song, Combination of acid-resistor and -scavenger improves the SEI stability and cycling ability of tin–nickel battery anodes in LiPF6-containing electrolyte, Electrochim. Acta 112 (2013) 252–257, https://doi.org/10.1016/j.electacta.2013.08.121, déc.
[28] C.-K. Kim, D.-S. Shin, K.-E. Kim, K. Shin, J.-J. Woo, S. Kim, S.Y. Hong, N.-S. Choi, Fluorinated hyperbranched cyclotriphosphazene simultaneously enhances the safety and electrochemical performance of high-voltage lithium-ion batteries, Chemelectrochem 3 (6) (2016) 913–921, https://doi.org/10.1002/celc.201600025.
[29] M. Xu, L. Hao, Y. Liu, W. Li, L. Xing, B. Li, Experimental and theoretical investigations of dimethylacetamide (DMAc) as electrolyte stabilizing additive for lithium ion batteries, J. Phys. Chem. C 115 (13) (2011) 6085–6094, https://doi.org/10.1021/jp109562u, avr.
[30] W. Li, C. Campion, B.L. Lucht, B. Ravdel, J. DiCarlo, K.M. Abraham, et al., Additives for stabilizing LiPF6-based electrolytes against thermal decomposition, J. Electrochem. Soc.,152 (2005) A1361, https://doi.org/10.1149/1.1926651.
[31] Z. Xiao, R. Wang, Y. Li, Y. Sun, S. Fan, K. Xiong, H. Zhang, Z. Qian, Electrochemical analysis for enhancing interface layer of spinel LiNi0.5Mn1.5O4 using p-toluenesulfonyl isocyanate as electrolyte additive, Front. Chem. 7 (2019). Consulté le: 9 mai 2023. [En ligne]. Disponible sur: https://www.frontiersin.org/articles/10.3389/fchem.2019.00591.
[32] W. P. Jencks, F. H. Westheimer, et R. Williams, « pKa Values », ACS, Organic Division.
[33] L. Chmurzyński, Studies on correlations of acid-base properties of substituted pyridine *N*-oxides in solutions. Part 1. Correlations of the p*K*a values in non-aqueous solvents and water, Anal. Chim. Acta 321 (2) (1996) 237–244, https://doi.org/10.1016/0003-2670(95)00594-3, mars.
[34] A. Wawrzynów, L. Chmurzyński, A comparison of acid – base properties of substituted pyridines and their N-oxides in propylene carbonate, J. Chem. Thermodyn. 30 (6) (1998) 713–722, https://doi.org/10.1006/jcht.1997.0337, juin.
[35] A. Guéguen, C. Bolli, M.A. Mendez, E.J. Berg, Elucidating the reactivity of tris (trimethylsilyl)phosphite and tris(trimethylsilyl)phosphate additives in carbonate electrolytes—a comparative online electrochemical mass spectrometry study, ACS Appl. Energy Mater. 3 (1) (2020) 290–299, https://doi.org/10.1021/acsaem.9b01551, janv.
[36] K. Kim, H. Ma, S. Park, N.-S. Choi, Electrolyte-additive-driven interfacial engineering for high-capacity electrodes in lithium-ion batteries: promise and challenges, ACS Energy Lett. 5 (5) (2020) 1537–1553, https://doi.org/10.1021/acsenergylett.0c00468, mai.
[37] Y.-M. Song, C.-K. Kim, K.-E. Kim, S.Y. Hong, N.-S. Choi, Exploiting chemically and electrochemically reactive phosphite derivatives for high-voltage spinel LiNi0.5Mn1.5O4 cathodes, J. Power Sources 302 (2016) 22–30, https://doi.org/10.1016/j.jpowsour.2015.10.043, janv.
[38] Y.-M. Song, J.-G. Han, S. Park, K.T. Lee, N.-S. Choi, A multifunctional phosphite-containing electrolyte for 5 V-class LiNi0.5Mn1.5O4 cathodes with superior electrochemical performance, J. Mater. Chem. A 2 (25) (2014) 9506–9513, https://doi.org/10.1039/C4TA01129E, juin.
[39] W.R. Wadt, W.A. Goddard, Electronic structure of pyrazine. Valence bond model for lone pair interactions, J. Am. Chem. Soc. 97 (8) (1975) 2034–2047, https://doi.org/10.1021/ja00841a008, avr.
[40] F. Polo-Garzon, Z. Wu, Acid–base catalysis over perovskites: a review, J. Mater. Chem. A 6 (7) (2018) 2877–2894, https://doi.org/10.1039/C7TA10591F, févr.
[41] V. Folliard, G. Postole, J.-F. Devaux, J.-L. Dubois, L. Marra, A. Auroux, Oxidative coupling of a mixture of bio-alcohols to produce a more sustainable acrolein: an in depth look in the mechanism implying aldehydes co-adsorption and acid/base sites, Appl. Catal. B Environ. 268 (2020) 118421, https://doi.org/10.1016/j.apcatb.2019.118421 juill.
[42] A.C. Martinez, S. Rigaud, S. Grugeon, P. Tran-Van, M. Armand, D. Cailleu, S. Pilard, S. Laruelle, Chemical reactivity of lithium difluorophosphate as electrolyte additive in LiNi0.6Co0.2Mn0.2O2/graphite cells, Electrochim. Acta 426 (2022) 140765, https://doi.org/10.1016/j.electacta.2022.140765 sept.
[43] « Case study: Pyridine Chemisorption analysis service for characterisation of acid sites ». Stoli Catalysts. [En ligne]. Disponible sur: https://stolichem.com/wp-content/uploads/2021/04/Pyridine-Desorption-Case-Study.pdf.
[44] K. Park, S. Yu, C. Lee, et H. Lee, Comparative study on lithium borates as corrosion inhibitors of aluminum current collector in lithium bis(fluorosulfonyl)imide electrolytes, J. Power Sources 296 (2015) 197–203, https://doi.org/10.1016/j.jpowsour.2015.07.052, nov.
[45] S. Zhou, S. Zhang, S. Wang, W. Zhang, Y. Liu, H. Lin, J. Chen, L. Yan, F. Zhang, H. Li, et H. Zheng, Direct evidences for bis(fluorosulfonyl)imide anion hydrolysis in industrial production: pathways based on thermodynamics analysis and theoretical simulation, J. Power Sources 577 (sept. 2023) 233249, https://doi.org/10.1016/j.jpowsour.2023.233249.
[46] H.-B. Han, S.-S. Zhou, D.-J. Zhang, S.-W. Feng, L.-F. Li, K. Liu, W.-F. Feng, J. Nie, H. Li, X.-J. Huang, M. Armand, Z.-B. Zhou, Lithium bis(fluorosulfonyl)imide (LiFSI) as conducting salt for nonaqueous liquid electrolytes for lithium-ion batteries: physicochemical and electrochemical properties, J. Power Sources 196 (7) (2011) 3623–3632, https://doi.org/10.1016/j.jpowsour.2010.12.040, avr.
[47] B. Liao, H. Li, M. Xu, L. Xing, Y. Liao, X. Ren, W. Fan, L. Yu, K. Xu, W. Li, Designing low impedance interface films simultaneously on anode and cathode for high energy batteries, Adv. Energy Mater. 8 (22) (2018) 1800802, https://doi.org/10.1002/aenm.201800802.
[48] J. Liu, Z. Chen, S. Busking, K. Amine, Lithium difluoro(oxalato)borate as a functional additive for lithium-ion batteries, Electrochem. Commun. 9 (3) (2007) 475–479, https://doi.org/10.1016/j.elecom.2006.10.022, mars.
[49] S. Shui Zhang, An unique lithium salt for the improved electrolyte of Li-ion battery, Electrochem. Commun. 8 (9) (sept. 2006) 1423–1428, https://doi.org/10.1016/j.elecom.2006.06.016.
[50] B. Salomez, S. Grugeon, M. Armand, P. Tran-Van, S. Laruelle, Review—gassing mechanisms in lithium-ion battery, J. Electrochem. Soc. (2023), https://doi.org/10.1149/1945-7111/acd2fd.
[51] Z. Du, D.L. Wood, et I. Belharouak, Enabling fast charging of high energy density Li-ion cells with high lithium ion transport electrolytes, Electrochem. Commun. 103 (2019) 109–113, https://doi.org/10.1016/j.elecom.2019.04.013, juin.
[52] E.R. Logan, A. Eldesoky, E. Eastwood, H. Hebecker, C.P. Aiken, M. Metzger, J. R. Dahn, The use of LiFSI and LiTFSI in LiFePO $_4$/graphite pouch cells to improve high-temperature lifetime, J. Electrochem. Soc. 169 (4) (2022) 040560, https://doi.org/10.1149/1945-7111/ac67f9 avr.
[53] V. Sharova, A. Moretti, T. Diemant, A. Varzi, R.J. Behm, S. Passerini, Comparative study of imide-based Li salts as electrolyte additives for Li-ion batteries, J. Power Sources 375 (2018) 43–52, https://doi.org/10.1016/j.jpowsour.2017.11.045, janv.